Mine Planning and Equipment Selection (MPES) Conference 2010

Determination of fracture toughness of anisotropic rocks under water vapour pressure by Semi-Circular Bend (SCB) test

M Kuruppu, Y Obara and M Kataoka

Reference Number: 11

Contact Author: (Use "Author Details" style)

Full name	Mahinda Kuruppu
Position title	Senior lecturer
Organisation Name	Curtin University
Address	Locked Bag 30, Curtin University, Kalgoorlie, 6433
Phone	08 9088 6173
Fax	08 9088 6151
Mobile	0409 510 537
Email	m.kuruppu@curtin.edu.au

Determination of fracture toughness of anisotropic rocks under water vapour pressure by Semi-Circular Bend (SCB) test

M Kuruppu[1], Y Obara[2] and M Kataoka[3]

1. Senior lecturer, Curtin University, Locked Bag 30, Kalgoorlie, Western Australia 6433,
Email: m.kuruppu@curtin.edu.au

2. Professor, Kumamoto University, Kurokami, Kumamoto 860-8555, Japan,
Email:obara@kumamoto-u.ac.jp

3. Student, Kumamoto University, Kurokami, Kumamoto 860-8555, Japan,
Email: i24nuovo4secolo51@yahoo.co.jp

ABSTRACT (USE “HEADING 1” STYLE)

Failure of rock materials is a process of crack propagation. Crack initiation takes place when the crack tip stress intensity K reaches a critical value called fracture toughness, K_{1C}. The rock fracture toughness is known to be affected by the surrounding environment such as temperature, confining pressure and humidity. In order to examine the effect of humidity a series of semi-circular bend tests were performed under various water vapour pressures in a rock material that is known to be anisotropic. Water vapour promotes stress corrosion of rock and therefore the fracture toughness was found to have a decreasing trend with increasing water vapour pressure. The rate of decreasing the fracture toughness depends on the microcrack density that promotes the migration of water vapour into the rock. Also in an anisotropic rock the fracture toughness depends on the direction of crack in relation to the anisotropy of the rock material.

Keywords: rock fracture, fracture toughness, anisotropy, micro cracks

INTRODUCTION

Fracture mechanics deals with initiation and propagation of cracks subjected to a stress field. The applicable theories depend on the brittleness or the ductility of the material. The cracks in rocks can be pre-existing or newly induced due to increased loading. The crack propagation that occurs in geological formations is often brittle and unstable in nature. But cracks can also propagate slowly and is known as stable crack propagation. An example of rock fracture mechanics is the fracturing of a Brazilian rock disc specimen in diametral compression in the laboratory to determine the indirect tensile strength or fracture toughness of the rock. The fracturing of a rock specimen due to the action of cutting using a wedge-shaped cutting tool is another example of rock fracture mechanics. Hydraulic fracturing as used to determine the *in situ* stresses and dynamic rock fragmentation is a third example. A fundamental feature of rock fracture mechanics lies in its ability to establish the relationship between rock fracture strength to the geometry of crack or cracks and the fracture toughness, the most fundamental parameter in fracture mechanics describing the resistance to crack propagation. It follows that crack propagation is the major cause of material failure in many cases. Thus, assessment of fracture toughness is important to the understanding of the behaviour of structures involving rock materials. Fracture toughness tests differ from ordinary strength tests in rock mechanics by requiring specimens with well defined cracks. Rock fracture toughness has been applied as a parameter for classification of rock materials, an index for rock fragmentation of rock material property in the interpretation of geological features and in stability analysis of rock structures, as well as in modelling of fracturing of rock (Whittaker et al., 1992; Ouchterlony, 1986).

Fracture mechanics principles were originally developed for man-made materials such as metals. However large differences exist in basic material response of metals and rocks during fracturing. They may be summarized as follows:

- Stress state: Most rock structures are subjected to compression but not tension. Therefore rock materials are strong in compression but weak in tension. Rocks are often brittle in nature i.e. they break with small deformation. They usually break due to tension;
- Nature of rock fracture: Rocks break in a brittle manner, but without plastic flow;
- Fracture process zone: In metals, the process zone near the crack tip is plastic in nature. But in rocks the process zone is formed due to microcracking. They also display high degree of nonlinearity during deformation.

In rock fracture mechanics applications, there are two distinct types of engineering problems. One is concerned with the prevention of failure in which fracture growth or movement, along the pre-existing fractures, is prevented such as in connection with the stability improvement of excavated rock structures. The other is concerned with the generation and propagation of new fractures as in hydraulic fracturing, rock fragmentation by cutting, and in drilling and blasting to optimize fracture processes in individual areas. Failure of rock materials is a process of crack propagation. Crack initiation takes place when the crack tip stress intensity factor K reaches the critical value, called fracture toughness K_C. The rock fracture toughness is known to be affected by the surrounding environment, such as temperature, confining pressure and humidity. In order to examine the effect of temperature, the double torsion test was performed under a condition of temperature 20 to 400 $^{\circ}C$ and water vapour pressure 10^3 to 10^5 Pa for granite and gabbro

(Meridith and Atkinson, 1995). They showed that the fracture toughness of gabbro increases below $100\,^{\circ}C$ and decreases thereafter and at $400\,^{\circ}C$ it becomes 60 to 50% of that of $20\,^{\circ}C$. Granite also has similar characteristics. Al-Shayea *et al.* (2000) determined the fracture toughness of limestone at in-situ conditions of temperature and confining pressure. In order to examine the effect of water vapour, a series of semi-circular bending tests were performed under various water vapour pressures (Obara et al., 2006). It was shown that the fracture toughness of Kumamoto andesite is dependent on water vapour pressure.

The uniaxial compressive strength and the tensile strength of rock are mechanical properties similar to the rock fracture toughness. It is also known that they are dependent on the surrounding environment, particularly water vapour pressure in the atmosphere. The water vapour promotes stress corrosion of rock (Freiman, 1984). Therefore the strength decreases with increasing water vapour pressure. Jeong *et al.* (2007) showed that the uniaxial compressive strength and tensile strength of rock increase with decreasing water vapour pressure. However, considering the significance of the influence of moisture on rock properties such as fracture toughness further research is needed. In addition, some rock materials are anisotropic, which can result in properties such as fracture toughness depend on the orientation of cracks with respect to planes of anisotropy (Whittaker et al., 1992).

Several tests exist in order to examine of fracture toughness, namely Chevron Bend (CB) test (Ouchterlony, 1986), Single Edge Notched Round Bar in Bending (SENRBB) test (Ouchterlony, 1980), Short Rod (SR) test (Barker, 1977), Central Straight-Through Brazilian Disk (CSTBD) test (Atkinson et al., 1982), Central through Chevron-Notched Brazilian Disk (CCNBD) test (Fowell and Xu, 1993), and Semi-Circular Bend (SCB) test (Chong and Kuruppu, 1984). The International Society for Rock Mechanics (ISRM, 1988; ISRM, 1995) suggested CB, SR and CCNBD specimens as standards for fracture toughness measurement. Among many different testing methods for the fracture toughness, the SCB specimen is chosen for its simplicity of specimen preparation, and testing procedure. For these reasons the SCB specimen has been popularly used by many researchers to determine fracture toughness of geomaterials (Aglan et al., 2009; Chen et al. 2009; Mull et al., 2002).

Therefore, in this study, fracture toughness of anisotropic rock was measured using SCB specimens under water vapour pressure. Its dependence on anisotropy was also measured.

SEMI-CIRCULAR BEND (SCB) TEST

The geometry of the Semi-Circular Bend specimen is shown in Figure 1. Developed by Chong and Kuruppu (1984), this specimen is a typical rock core-based specimen requiring very little machining. It is made of slicing the core into disks and then splitting each disk into two halves to make two specimens having almost identical properties. This character is sometimes useful as the variation of fracture properties through a core length is usually significant. It is suitable for small, compact specimens requiring duplicate samples to investigate fracture toughness when subjected to changing parameters such as strain rate, confining pressure, moisture content and temperature. The fracture toughness K_{IC} is of the following form (Chong and Kuruppu, 1987):

$$K_{IC} = \frac{P_{\max}\sqrt{\pi a}}{2rt} Y_I \qquad (1)$$

Y_I is the dimensionless stress intensity factor shown in Figure 2 as a function of the dimensionless crack length *a/r* with r being half the disk diameter (Lim *et al*. 1993). Pmax is the maximum load attained before fracture and t is the thickness. The results of Figure 2 can be approximated by a third order polynomial as follows:

$$Y_I = 5.5634 - 11.219(a/r) + 17.687(a/r)^2 + 124.89(a/r)^3 - 364.54(a/r)^4 + 302.14(a/r)^5 \qquad (2)$$

Equation (2) is applicable for the span ratio s/r of 0.8 only. The half disk specimen can be also tested for mixed mode fracture toughness studies (Kuruppu and Chong, 1986). Researchers have used the SCB specimen to investigate mixed mode fracture by having an angled crack instead of a symmetric crack.

THE APPLICATION OF SCB TEST FOR FRACTURE TOUGHNESS MEASUREMENT OF ANISOTROPIC ROCK

A series of tests for the determination of fracture toughness of Africa Rutenburg granite was carried out at the laboratories of Kumamoto University in Western Japan. Figure 3 shows SCB specimen made of Africa Rustenberg granite and prepared for Mode 1 testing. This rock is composed of amphibole, plagioclass, pyroxene etc. which are investigated by qualitative analysis using X-ray diffraction.

In order to investigate the orientation of micro cracks, observation of a thin section of this rock was performed using polarization microscope. Figure 4 shows a photograph of the thin section which shows that the grain boundaries are mostly aligned with x-axis. Axes x and *y* in this figure are defined arbitrarily and x-direction is aligned with Axis-3 of the frame of reference. In order to count the distribution of micro crack orientation, the strike of each micro crack is measured and its frequency is summarized in the rose diagram with an interval of 20 degrees as shown in Figure 5. This result shows that the many micro cracks are almost oriented between 100 and 120 degrees from x-axis.

This rock is known as anisotropic and has been tested for elastic wave velocity in three perpendicular directions (Figure 6). The results show that the elastic wave velocity is the same in two directions. However it is different in the third direction, which confirms that Africa Rustenburg granite is a transversely isotropic material. On the basis of the results, the three directions were defined as Axis-1, Axis-2 and Axis-3, and planes perpendicular to each axis were defined as Plane-1, Plane-2 and Plane-3. The elastic wave velocity in Plane-1 is approximately equal considering two perpendicular directions in that plane with *Vp*=6575m/s and 6543m/s. However the elastic wave velocity measured in a direction perpendicular to Plane-1 is higher (*Vp*=6757m/s). That direction has a lower resistance to elastic wave propagation perhaps showing lower micro crack density in Plane-1 compared to that in Plane-2 and Plane-3. The micro cracks in Plane-1, Plane-2 and Plane-3 are called Crack-1, Crack-2 and Crack-3 respectively for the purpose of identification.

The material exhibits two groups of inherent cracks. The two groups of Crack-2 and Crack-3 are oriented perpendicular to Axis-2 and Axis-3 respectively. They have the same intensity of crack and therefore the elastic wave velocity is found to be the same. The group of Crack-1 which is oriented perpendicular to Axis-1 has higher elastic wave velocity. Therefore the intensity of cracks is less than that in the other two groups. In this study, two types of SCB specimens were prepared, 1-2 type and 3-2 type (Figure 7). The first figure defines the direction of propagation of the crack. The second figure defines the plane of the specimen. The artificial notch in each specimen has been chosen to represent natural cracks having that plane and direction.

SCB specimen is made from typical rock core approximately 75 mm in diameter. The core is sliced into disks of approximately 20 mm thickness and then split into two halves. The specimens were machined using a diamond coated, circular disk cutter. An artificial notch was made by a diamond blade with a thickness of 0.4 mm. The crack length ratio a/r = 0.5 where a and r are defined in Figure 3. It is necessary that water in specimen is removed to examine influence of surrounding environment of rock. In order to achieve complete dry condition of the rock specimens, they were kept in the electric drier oven at 100 $^{\circ}C$ for more than 30 days.

EXPERIMENT PROCEDURE

Experimental system

The setup of specimen for SCB test is shown in Figure 8. Test specimen is placed on two lower support rollers with support span width 2*s* and the span ratio s/r is 0.8. The load is applied through one upper and two lower rollers. Loading plate with load cell can move up and down vertically by guide rods.

Figure 9 shows a vacuum chamber used in the test to control surrounding environment of rock specimen. The chamber, which is made of SUS304 steel, has upper and lower flanges with a rod for compression, and six ports and a valve to inject the gases. Two of the ports are used to lead the output from strain gauges pasted to the specimen surface. Another two ports are to measure the vapour pressure in the chamber by two types of pressure gauges. One port is the window for observing inside of the chamber and the last port

with a valve is connected to the air evacuation system through a flexible tube. During the test, the chamber is linked to the vacuum system that is used to introduce the required level of vapour pressure.

The specimen is placed on a loading plate inside the vacuum chamber. The chamber along with the specimen is placed in a MTS servo-controlled testing machine having a capacity of 100 kN as shown in Figure 10. The flanges of the chamber are supported by two columns with springs (Figure 11). These springs prevent any load application on the specimen while the vapour pressure is controlled before the start of the test. Load and displacement data during the test is measured by a load cell with a capacity of 10 kN and a displacement gauge connected to the test specimen.

In this test, it is necessary that the air in the chamber is removed along with water vapour. Subsequently, we introduced various quantities of water vapour as required for testing. The evacuation system consists of two pumps, a rotary pump and a turbo molecular pump. The water vapour pressure is measured using two gauges. One is APGX pressure gauge with a measurement range of 10^{-1} to 10^{5} Pa and the other is AIMS pressure gauge with a measurement range of 10^{-6} to 10^{0} Pa, both shown Figure 12. Pressure data measured by these gauges is recorded as a voltage through a control panel.

Testing method

SCB specimen is wiped dirt using acetone. The environmental chamber with the specimen placed inside is set up on the MTS testing machine. The specimen is loaded via a rod passing through the upper flange of the chamber. Tests were performed at a constant displacement rate of 0.01 mm/min. The water vapour pressure is controlled before testing as described below.

Figure 13 shows the change of pressure in the chamber during test. The air in the chamber is removed using the two vacuum pumps until the pressure dropped to less than 10^{-2} Pa. Distilled water is then injected through the injection valve to a pressure of about 10^{3} Pa. As a result, the pressure in the chamber becomes the saturated water vapour pressure and the chamber is filled with only water vapour. Subsequently the water vapour in the chamber is exhausted until reaching the pressure required for the test. This water vapour pressure is maintained for about 6 hours before the fracture toughness test is performed.

RESULTS AND DISCUSSION

Table 1 shows results of fracture toughness tests of Africa Rustenberg granite. SCB tests were performed on 11 specimens of 1-2 type and 14 specimens of 3-2 type. The range of water vapour pressure in the test is from 8.4×10^{-2} Pa to 7.7×10^{2} Pa. The fracture toughness K_{IC} is calculated by equation (1).

Figure 14 shows a fractured specimen after test. The crack propagated straight from the edge of artificial notch to the upper loading point. Figure 15 gives an example of load-displacement curve of a test done at the vapour pressure shown in the figure. This curve is downward convex at low stress level, and is linear until specimen failed at maximum load. The relation between fracture toughness K_{IC} and water vapour pressure is shown in Figure.16. The vertical axis is fracture toughness and the horizontal axis is water vapour pressure, and both axes are logarithmic. The values of fracture toughness of 1-2 type are larger than those of 3-2 type. This shows that rock fracture toughness depends on anisotropy. The fracture toughness of both types varies almost linearly against water vapour pressure and they have a decreasing trend. Lines drawn using least square approximation are also shown. The equation of those lines is represented as:

$$K_{IC} = \beta p^{-m} \tag{3}$$

where β is a constant and *m* is the negative slope of the approximated line on the logarithmic graph. The parameter *m* is 0.0307 for 1-2 type and 0.0097 for 3-2 type. As the m-value for 1-2 type is larger than for 3-2 type, the influence of water vapour pressure to fracture toughness for 1-2 type may be stronger than that for 3-2 type.

3-2 type specimens which have the notch cracks in Plane-1 may be fractured by the effect of grain boundaries, which are oriented in the same plane. Conversely 1-2 type specimens require fracturing through the gains while overcoming greater resistance. A microstructural study of rock materials has shown that intergranular cracks (grain boundary cracks) and transgranular cracks (cracks cut across mineral grains) are present in rock materials (Whittaker et al, 1992). However they may have different resistance to fracture. From this and the observed results, it is found that the fracture toughness depends on the orientation of the artificial crack with respect to the material inhomogeneity. This also explains the difference of *m* value

between Africa Rustenberg granite 1-2 type and 3-2 type. Microcracks are known as planes of weakness in a rock. The effect of stress corrosion on such planes can be significant thus reducing the resistance to crack propagation rapidly. Therefore water vapour migrated through the dense array of microcracks has a greater influence on the fracture resistance of 1-2 type making the m value larger.

CONCLUSIONS

Africa Rustenberg granite has isotropic properties in one plane (Plane-1) but the properties in the other two major planes are different from those of Plane-1. Hence its properties are close to transversely isotropic. Both the elastic wave velocity and the fracture toughness showed the directional dependence. The measured elastic wave velocity was lower in both major directions of Plane-1 as there is a high microcrack density in perpendicular planes. When the fracture toughness was measured in a plane perpendicular to Plane-1 (e.g. 1-2 type), it was found to be higher than when the notch cracks were oriented in Plane-1. Moreover, the logarithmic graph of K_{IC} versus water vapour pressure shows a distinctly different gradient for 1-2 type in comparison with that for 3-2 type. This can be explained by the increase in fracture resistance in a direction perpendicular to the orientation of grain boundaries, and the facilitation of rapid stress corrosion due to the higher density of microcracks. Therefore the fracture toughness of Africa Rustenberg granite depends on both the parameters investigated in this study, namely the water vapour pressure and the orientation of the crack with respect to the microstructural anisotropy of the material.

ACKNOWLEDGEMENTS

One of the authors (MK) thankfully acknowledges the fellowship offered by Japanese Society for the Promotion of Science to visit the rock fracture mechanics research group in Kumamoto University, Japan.

REFERENCES

Aglan, H. Morsy, M, Allie, A and Fouad, F, 2009. Evaluation of fiber reinforced nanostructured perlite-cementitious surface compounds for building shin applications, in *Construction and Building Materials*, Vol. 23, pp 138-145 (Elsevier).

Al-shayea, N A, Khan, K and Abduljauwad, S N, 2000. Effects of confining pressure and temperature on mixed-mode (I-II) fracture toughness of a limestone rock, *Int. J. Rock Mech. Min. Sci.*, 37, pp 629-643.

Atkinson, C, Smelser, R E and Sanchez, J, 1982. Combined mode fracture via the cracked Brazilian disk test, *Int. J. Fract.*, Vol. 18, No.4, pp.279-291.

Barker, L M, 1977. A simplified method for measuring plane-strain fracture toughness, *Eng. Fract. Mech.*, 9:361-369.

Chen, R, Xia, K, Dai, F, Lu, F and Luo, S N, 2009. Determination of dynamic fracture parameters using a semi-circular bend technique in split Hopkinson pressure bar testing, in *Eng. Fracture Mech.*, 76:1268-1276, (Elsevier).

Chong, K.P. and Kuruppu, M.D.: New specimen for fracture toughness determination for rock and other materials, *Int. J. Fract.*, 26, R59-62, 1984.

Chong, K P and Kuruppu M D, 1987. Fracture toughness determination of layered materials, *Eng. Fract. Mech*., Vol.28, No.1, pp.43-54.

Fowell, R J and Xu C, 1993. The cracked Chevron notched Brazilian disc test – geometrical considerations for practical rock fracture toughness measurement, *Int. J. Rock Mech. Min. Sci. Geomech. Abstr*., 30:821-824.

Freiman, S W, 1984. Effects of chemical environments on slow crack growth in glasses and ceramics, *J. Geophys. Res.*, 89:4072-4076.

ISRM Testing Commission, (Ouchterlony, F. Co-ordinator), 1988. Suggested methods for determining the fracture toughness of rock, *Int. J. Rock Mech. Min. Sci. & Geomech. Abstr*., 25:71-96.

ISRM Testing commission, Fowell, R J, 1995. Suggested method for determining mode-I fracture toughness using cracked Chevron notched Brazilian disk (CCNBD) specimens. *Int. J. Rock Mech. Min. Sci.Geomech. Abstr.*, 32:57-64.

Jeong, H S, Kang, S S and Obara, Y, 2007. Influence of surrounding environments and strain rates on strength of rocks under uniaxial compression, *Int. J. Rock Mech. Sci.*, 44:321-331.

Kuruppu, M D and Chong, K P, 1986. New specimens for modes I and II fracture investigations of geometries, *Proc. Soc. Expl. Mech*., Spring Conf. on Expl. Mech., New Orleans, U.S.A., pp.31-38.

Lim, I L, Johnston, I W and Choi, S K, 1993. Stress intensity factors for semi-circular specimens under three-point bending, *Engng. Fract. Mech*., 44:363-382.

Meredith, P G and Atkinson, B K, 1985. Fracture toughness and subcritical crack growth during high-temperature tensile deformation of Westerly granite and Black gabbro, *Phys. Earth Planet. Int.*, 39:33-51.

Mull, M A, Stuart, K and Yehia, A, 2002. Fracture resistance characterisation of chemically modified crumb rubber asphalt pavement, in *J of Materials Sci.*, Vol. 37, pp 557-566 (Kluwer Academic Publ.).

Obara, Y, Sasaki, K, Matusyama, T and Yoshinaga, T, 2006. Influence of water vapor pressure of surrounding environment on fracture toughness of rock, *Proc. of ARMS- Asian Rock Mechanics Symposium*, CD-7 chapter.

Oucterlony, F, 1986. A core bend specimen with chevron notch for fracture toughness measurements, Rock Mechanics: Key to Energy Production, *Proc. 27th U. symp. on Rock Mech.*, H.L. Hartman, (Ed.), Littleton Co., pp.177-184 (SME).

Ouchterlony, F, 1980. A New Core Specimen for the Fracture Toughness Testing of Rocks, *Swedish Detonic Research Foundation Rep. DS, P10,* Stockholm, Sweden.

Whittaker, B N, Singh, R N and Sun, G, 1992. Rock Fracture Mechanics, Principles, Design and Applications, Developments in Geotechnical Engineering, 71.

FIGURE CAPTIONS

Fig 1 – Semi-circular bend (SCB) specimen.

Fig 2 – Mode I normalised Stress intensity factor of SCB specimen.

Fig 3 – SCB specimen made of Africa Rutenburg granite

Fig 4 – A thin section micrograph of Africa Rutenburg granite

Fig 5 – Rose diagram showing the frequency of microcrack orientation.

Fig 6 – Elastic wave velocity in 3 perpendicular directions.

Fig 7 - Preparation of specimens using a core drilled in the direction of Axis-2.

Fig 8 – Set up of specimen for testing

Fig 9 – Vacuum chamber.

Fig 10 - MTS testing system.

Fig 11 – Set up of the chamber supported by two steel columns with springs.

Fig 12 – Schematic view of air evacuation system.

Fig 13 – Pressure in the chamber during testing.

Fig 14 – Photograph of a fractured specimen of Africa Rustenberg granite.

Fig 15 – A typical load-displacement curve.

Fig 16 – Relationship between fracture toughness and water vapour pressure.

TABLE CAPTIONS

Table 1. Fracture toughness and water vapour pressure for Africa Rustenberg granite.

FIGURES

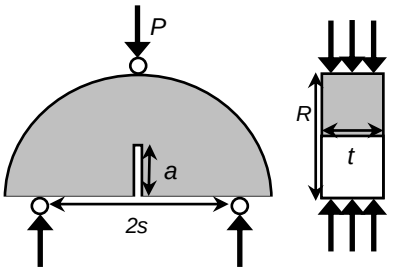

Fig 1 – Semı-circular bend (SCB) specimen.

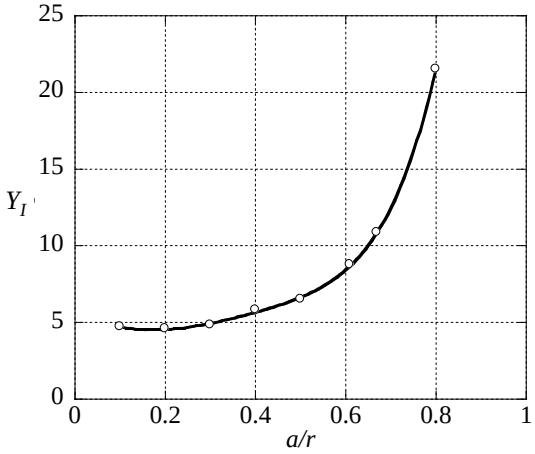

Fig 2 – Mode I normalised Stress intensity factor of SCB specimen.

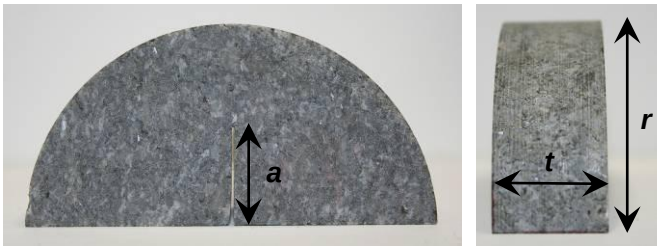

Fig 3 – SCB specimen made of Africa Rutenburg granite.

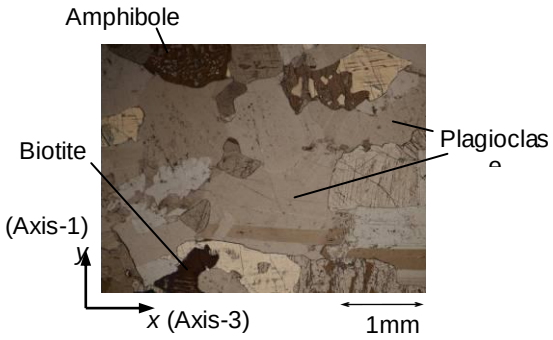

Fig 4 – A thin section micrograph of Africa Rutenburg granite.

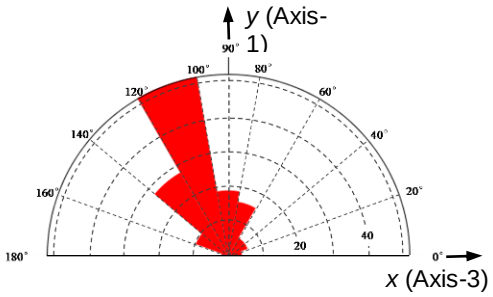

Fig 5 – Rose diagram showing the frequency of microcrack orientation.

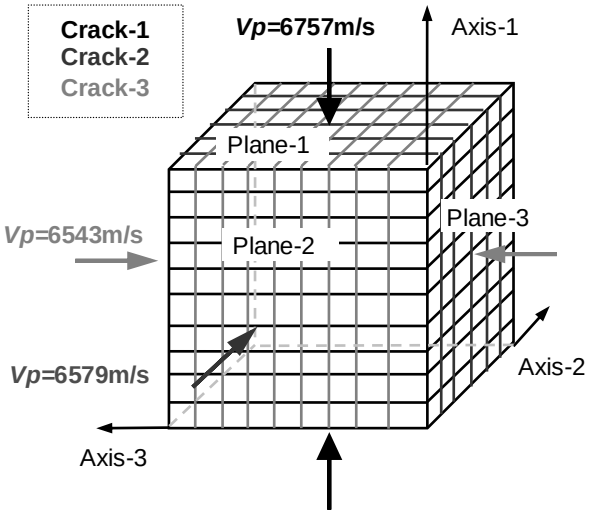

Fig 6 – Elastic wave velocity in 3 perpendicular directions.

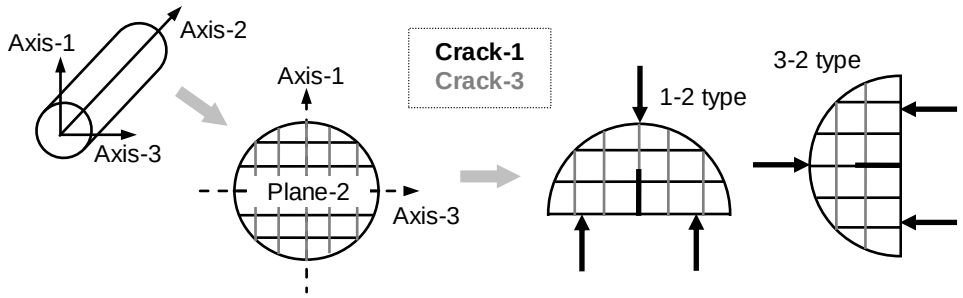

Fig 7 - Preparation of specimens using a core drilled in the direction of Axis-2.

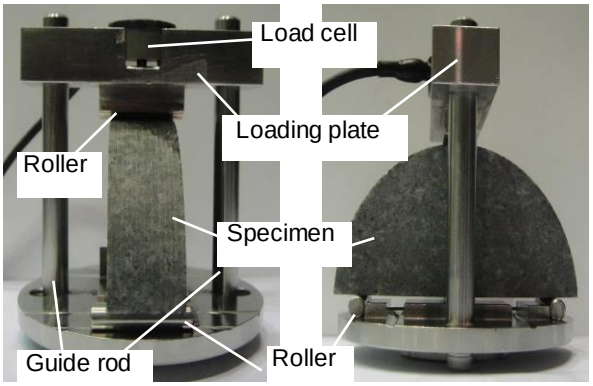

Fig 8 – Set up of specimen for testing

Fig 9 – Vacuum chamber.

Fig 10 - MTS testing system.

Fig 11 – Set up of the chamber supported by two steel columns with springs.

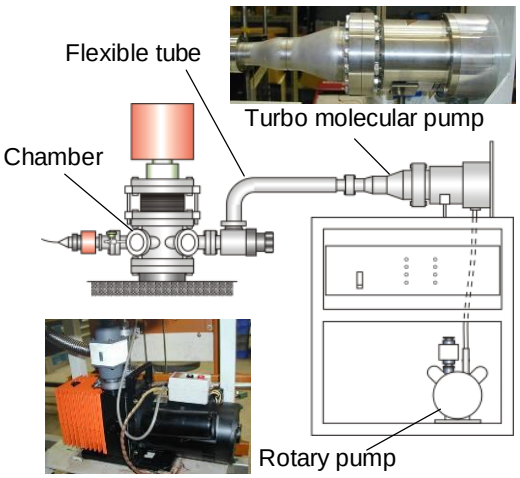

Fig 12 – Schematic view of air evacuation system.

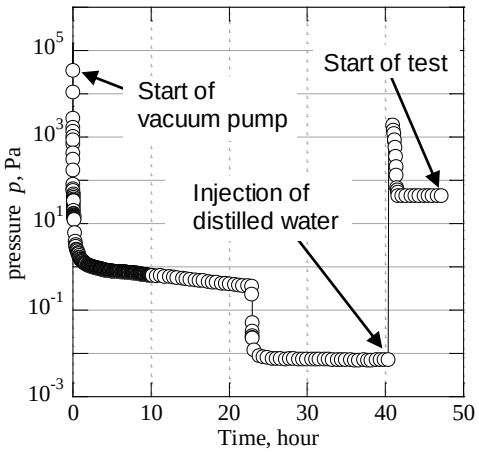

Fig 13 – Pressure in the chamber during testing.

Fig 14 – Photograph of a fractured specimen of Africa Rustenberg granite.

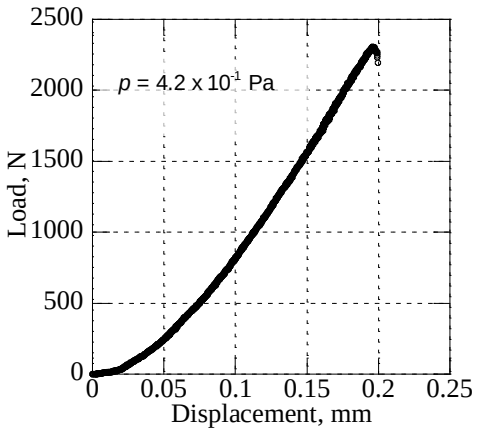

Fig 15 – A typical load-displacement curve.

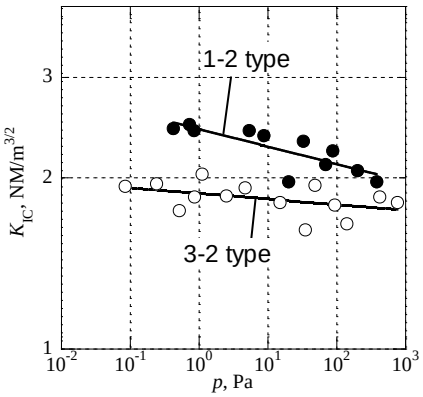

Fig 16 – Relationship between fracture toughness and water vapour pressure.

TABLES

Table 1. Fracture toughness and water vapour pressure for Africa Rustenberg granite.

Type	No.	Water vapor pressure p(Pa)	Fracture toughness K_{IC}(MN/m$^{3/2}$)
1-2	1	4.2 x 10^{-1}	2.44
1-2	2	7.2 x 10^{-1}	2.48
1-2	3	8.5 x 10^{-1}	2.42
1-2	4	5.4 x 10^{0}	2.42
1-2	5	8.7 x 10^{0}	2.37
1-2	6	1.6 x 10^{1}	1.97
1-2	7	3.3 x 10^{1}	2.32
1-2	8	6.9 x 10^{1}	2.11
1-2	9	8.7 x 10^{1}	2.23
1-2	10	2.0 x 10^{2}	2.06
1-2	11	3.8 x 10^{2}	1.97

Type	No.	Water vapor pressure p(Pa)	Fracture toughness K_{IC}(MN/m$^{3/2}$)
3-2	1	8.4 x 10^{-2}	1.93
3-2	2	2.4 x 10^{-1}	1.95
3-2	3	5.2 x 10^{-1}	1.75
3-2	4	8.6 x 10^{-1}	1.85
3-2	5	1.1 x 10^{0}	2.03
3-2	6	2.5 x 10^{0}	1.86
3-2	7	4.7 x 10^{0}	1.92
3-2	8	1.5 x 10^{1}	1.81
3-2	9	3.5 x 10^{1}	1.62
3-2	10	4.8 x 10^{1}	1.94
3-2	11	9.3 x 10^{1}	1.79
3-2	12	1.4 x 10^{2}	1.66
3-2	13	4.2 x 10^{2}	1.85
3-2	14	7.7 x 10^{2}	1.81